JOURNAL OF SOLID STATE CHEMISTRY 1, 409–418 (1970)

The System $SrMnO_{3-x}$

TAKI NEGAS AND ROBERT S. ROTH

National Bureau of Standards, Washington, D.C. 20234

Received October 9, 1969

The system $SrMnO_{3-x}$ ($0 \leq x \leq 0.5$) was investigated by gravimetric and quenching experiments. Four-layer, hexagonal $SrMnO_3$ ($a = 5.449$ Å, $c = 9.078$ Å) is stable in air below 1035°C. Above 1035°C the basic structure becomes increasingly anion deficient, reaching the limiting composition $SrMnO_{2.89}$ near 1400°C. Unit cell dimensions increase and distortion to orthorhombic symmetry occurs with decreasing oxygen content. Further reduction occurs from 1400°C to a melting point at 1740°C and a "perovskite" homogeneity range exists with limits $SrMnO_{2.74}$ and $SrMnO_{2.62}$. The anion-deficient perovskite phases can be rapidly reoxidized at low temperatures to yield a metastable cubic perovskite, $SrMnO_3$ ($a = 3.806$ Å). Stoichiometry and stability of phases are discussed from the standpoint of variation in the coordination of the manganese cation.

Introduction

The ABO_3 compounds (A = alkaline earth, B = transition metal) are of particular interest because of their potentially useful magnetic and electrical properties. Unfortunately, the characterization of such materials through phase equilibria and X-ray diffraction studies is difficult because of the tendency of the B ion to exist within a given phase in mixed oxidation states. Therefore, at a constant oxygen pressure, phases of fixed A–B ratio may appear to exist over a wide, temperature-dependent, oxygen homogeneity range. Generally, such phases are regarded as nonstoichiometric or disordered, defect, solid solutions. True compounds result if long-range ordering of defects is accomplished.

Wadsley (*1*) has extensively discussed these considerations and expressed personal interest in this study of $SrMnO_{3-x}$ as well as ABO_{3-x} systems in general. He emphasized the importance of transition metal–oxygen mixed coordination schemes associated with anion deficient phases. Although difficult to detect in close-packed oxide systems unless completely ordered [Gorter (2)], coordination provides a useful framework from which variation of structure with stoichiometry can be best understood and reconciled.

Several phases with the 1:1 Sr–Mn ratio in the system SrO-"manganese oxide" were prepared at elevated temperatures in air and vacuum. The influence of stoichiometry is suggested by the stability and structure of these phases.

Although $SrMnO_3$ has been used extensively in magnetic studies (*3*) and (*4*) involving solid solutions with $LaMnO_3$ and $CaMnO_3$, very little is known about the isolated material. Jonker and Van Santen (*3*) prepared nearly stoichiometric $SrMnO_3$ at an unspecified temperature and oxygen pressure. They also synthesized a similar phase at 1350°C in air but this specimen contained only 85% Mn^{4+} (which can be written as $SrMnO_{2.925}$). Published X-ray powder data for $SrMnO_3$ are lacking although Jonker and Van Santen indicated that the phase is definitely not of the perovskite type. It is noteworthy that of the first-row transition metals only nickel and manganese have not been reported to form perovskite-like oxide phases with strontium.

Experimental Procedure

Weighed amounts of $SrCO_3$ and MnO_2 were hand mixed under acetone, packed in a gold envelope, and calcined in air for 2 weeks each at 800 and 1000°C. This treatment was sufficient to remove all of the available carbonate. The product was then calcined on Pt-foil at 1250°C in air for 2 weeks and then slow-cooled to room temperature. Calcined specimens were equilibrated in air and in vacuum using the quench method. For experiments conducted below 1700°C in air, a vertical-tube resistance-type furnace was used. A similar furnace, modified for vacuum capability, was used for a limited number of lower-oxygen-pressure experiments. In these furnaces, temperatures were measured with Pt–Pt 10% Rh thermocouples calibrated against

the melting points of NaCl (801°C), Au (1063°C), and Pd (1552°C). For experiments conducted above 1700°C in air, a quench furnace previously described (*5*) was used. Temperatures were measured in this furnace with a calibrated, disappearing filament-type, optical pyrometer which was sighted through a 45° calibrated prism into the hot-zone of the furnace. This system was calibrated against the melting points of Pd and Pt (1769°C). All furnaces were controlled by a-c Wheatstone bridge instruments capable of maintaining temperature to at least ±2°C.

X-Ray powder patterns of specimens were made at room temperature using a high-angle Geiger counter-diffractometer and Ni-filtered Cu radiation. The scanning rate was $\frac{1}{4}°$ 2θ/min. Unit cell dimensions were refined by a least-squares computer program and are estimated to be accurate to at least ±2 in the last decimal place listed. Gravimetric data were obtained from 1.5- to 2-g specimens, which had previously been equilibrated at a desired temperature and quenched in solid CO_2 or water. These specimens were weighed at room temperature, then heated in air at a temperature near 800°C, or in some cases to 300°C. The specimens were removed from the furnace and reweighed after cooling. This procedure, therefore, involves the reversal of a high-temperature reduced phase to a known low-temperature oxidized phase.

Experimental Results

The air (ambient pressure) isobar in the system $SrMnO_{3-x}$, between $x = 0$ to $x = 0.5$, is shown in Fig. 1, which was constructed from the quenching and gravimetric data in Table I. Results are expressed in terms of the formula $SrMn_2^{3+}Mn_{1-2x}^{4+}O_{3-x}$. Important features of Fig. 1 will be discussed individually in following sections. Broad features, however, include:

(a) a homogeneity range with limits $SrMnO_3$ ($x = 0$) to near $SrMnO_{2.89}$ ($x = 0.11$) at approximately 1400°C;

(b) a "phase transition" near 1400°C;

(c) a second homogeneity range with limits near $SrMnO_{2.74}$ at 1400°C and approximately $SrMnO_{2.62}$ near 1740°C;

(d) melting, with oxygen loss at 1740°C.

Hexagonal $SrMnO_3$

The compound $SrMnO_3$ is stable in air below 1035°C. Its X-ray diffraction pattern, given in Table II, was indexed on the basis of a hexagonal cell with $a = 5.449$ Å and $c = 9.078$ Å. Superstructure and extraneous lines due to impurities are absent and the pattern is quite well-defined with no evidence of distortion from hexagonal symmetry. Material heated at 1000°C and in an O_2 environment (~70 atm) showed no changes in lattice parameters. These data, as well as the similarity of corresponding line intensities, suggest that $SrMnO_3$ is isostructural with the high temperature form of $BaMnO_3$ (*6*), hexagonal, $a = 5.669$ Å, $c = 9.38$ Å, space group $P6_3/mmc$. Katz and Ward (*7*) reported that, "an unpublished report by Paul Braun indicates that $SrMnO_3$ has the $BaMnO_3$ structure." Both high-temperature $BaMnO_3$ and low-temperature $SrMnO_3$ consist of four close-packed AO_3 (A = Sr or Ba) layers in an ABAC (4L, L = layer) stacking sequence. Tetravalent Mn assumes interlayer octahedral sites. Oxygen octahedra containing Mn^{4+} are grouped into face-sharing pairs linked by corner-sharing within the cubically stacked A layers. Low-temperature $SrMnO_3$ is the only known Sr derivative of the ABO_3 type which features face-sharing of filled octahedra.

$BaMnO_3$ also exists in a low-temperature modification (*6*) apparently isostructural with

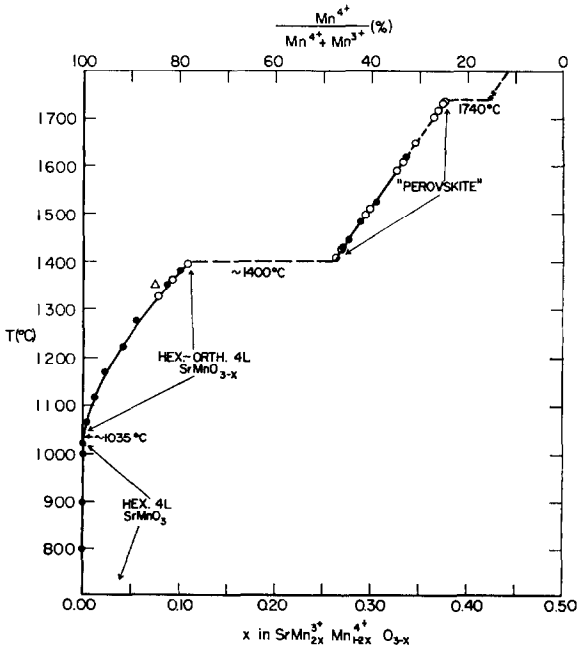

FIG. 1. The air isobar in the system $SrMnO_{3-x}$. [4L = four-layer structure; △ Jonker and Van Santen (*3*); ▲ $SrMnO_{2.558}$ prepared in vacuum, perovskite-like; ● single phase solid, gravimetrically determined; ○ single phase solid; ◑ two solid phases, incomplete reaction; * liquid, composition shown schematically.]

TABLE I

EXPERIMENTAL DATA FOR THE SYSTEM $SrMnO_{3-x}$[a]

Temp (°C)	Time (h)[b]	X-ray diffraction analysis[c]	X in $SrMnO_{3-x}$[d]	Remarks
350	223	4L		
650	65	4L		
800	72	4L		
900	20	4L		
1000	110	4L	0	
1000	5	4L		~70 atm O_2
1021	475	4L	0	
1067	261	4L (reduced)	0.004	
1117	215	4L (reduced)	0.012	
1169	258	4L (reduced)	0.022	
1222	216	4L (reduced)	0.042	
1274	213	4L (reduced)	0.056	
1325	428	4L (reduced)		
1350	216	4L (reduced)	0.087	
1360	336	4L (reduced)		
1381	235	4L (reduced)	0.101	
1395	120	4L (reduced)		
1408	63	4L (reduced) + P[e]		
1426	213	4L (reduced) + P[e]		
1431	382	4L (reduced) + P[e]		
1445	261	P	0.276	
1482	95	P	0.289	
1498	4	P		
1510	70	P		
1525	17	P	0.306	
1591	2	P		
1609	64	P		
1619	5	P	0.336	
1649	2	P		
1704	3	P		
1718	1	P		
1733	1	P		
1736	1	P		
1744	1	P		Melted
1751	1	P		Melted
800	99	4L	0[f]	Reheat of $SrMnO_3$ cubic perovskite
1000	34	4L		Reheat of 1510°C specimen
1150	168	P	0.442	6×10^{-6} atm
1175	168	P		3×10^{-5} atm
1340	168	?		5×10^{-6} atm

[a] In air unless otherwise indicated.

[b] Does not include previous calcines. Starting material prepared by heating 2 weeks each at 800 and 1000°C plus 2 weeks at 1250°C and slow-cooled in air.

[c] Determined at room temperature. 4L = four-layer phase, $SrMnO_3$. 4L (reduced) = four-layer $SrMnO_{3-x}$. P = perovskite-like, $SrMnO_{3-x}$.

[d] For 4L (reduced) phases, determined by reoxidation at 800–900°C to 4L $SrMnO_3$. For P phases, determined by reoxidation at 300°C to cubic perovskite, $SrMnO_3$.

[e] Incomplete, sluggish conversion to P phase.

[f] Metastable cubic perovskite to hexagonal, 4L $SrMnO_3$ involves no weight change.

? Unknown phase.

TABLE II

X-RAY DIFFRACTION DATA FOR HEXAGONAL, LOW-TEMPERATURE, FOUR-LAYER $SrMnO_3$

d_{obs}[a]	I/I_1[b]	$1/d^2_{calc}$	$1/d^2_{obs}$	hkl[c]
4.719	5	0.0449	0.0449	100
4.185	2	0.0570	0.0571	101
3.270	60	0.0935	0.0935	102
2.723	100	0.1348	0.1348	110
2.547	45	0.1541	0.1541	103
2.283	10	0.1918	0.1918	201
2.269	10	0.1941	0.1941	004
2.093	45	0.2282	0.2282	202
2.045	10	0.2391	0.2391	104
1.8607	30	0.2889	0.2889	203
1.7437	2	0.3289	0.3289	114
1.6947	5	0.3482	0.3482	105
1.6598	10	0.3629	0.3630	212
1.6359	5	0.3738	0.3737	204
1.5730	20	0.4042	0.4042	300
1.5499	2	0.4164	0.4163	301
1.5364	20	0.4236	0.4236	213
1.4409	10	0.4818	0.4817	106
1.4389	10	0.4830	0.4830	205
1.4023	5	0.5086	0.5086	214
1.3622	25	0.5390	0.5390	220
1.2736	10	0.6165	0.6165	206
1.2723	10	0.6177	0.6178	215
1.2576	5	0.6325	0.6323	312
1.2012	5	0.6931	0.6931	313
1.1680	2	0.7331	0.7331	224
1.1537	5	0.7512	0.7513	216
1.1417	5	0.7671	0.7671	402
1.1347	2	0.7766	0.7766	008

[a] Interplanar spacing, Å.

[b] Relative intensity.

[c] Indexed on the basis of a hexagonal cell with $a = 5.449$, $c = 9.078$

$BaNiO_3$ (*8*) and $BaCoO_{3-x}$ (*9*). The structure of $BaNiO_3$ has been proposed to consist of close-packed layers in an AB (hex 2L) sequence, with the transition metal occupying octahedra, all of which share faces (*8*). It is interesting to speculate as to why $SrMnO_3$ does not form this structure or the perovskite structure (ABC sequence) which is related to the high and low forms. In high $BaMnO_3$ each BaO_3 layer is approximately 2.35 Å thick, providing for a distance of about 2.62 Å between the Mn^{4+} cations in face-sharing octahedral sites (*6*). Each SrO_3 layer, however, is roughly 2.27 Å thick, which allows a Mn–Mn distance of about 2.54 Å. The distances between transition metals in octahedra which share corners in high $BaMnO_3$ and $SrMnO_3$ are 3.88 Å and approximately 3.81 Å, respectively. The shorter Mn–Mn distances probably reflect structural stabilization by Mn–Mn interaction through overlap of d orbitals and/or by increased oxygen polarization. The 2.54 Å distance appears long enough to allow the attractive terms to dominate. The low $BaMnO_3$ structure ($a = 5.67$ Å, $c = 4.71$ Å), is characterized by even shorter Mn–Mn distances of approximately $\frac{1}{2}c$ or 2.35 Å. Similarly, isotypes $BaCoO_{3-x}$ and $BaNiO_3$ contain metal–metal distances of 2.39 and 2.42 Å, respectively. If $SrMnO_3$ were to assume the 2L structure, the approximate cell dimensions could be predicted from a knowledge of the high-form parameters and the relations among cell dimensions, layer thickness, and cation–cation distances of the Ba forms. Hexagonal 2L $SrMnO_3$ would have the maximum parameters of $a \approx 5.45$ Å and $c \approx 4.54$ Å. The resulting Mn–Mn distance would be approximately $\frac{1}{2}c$ or 2.27 Å, a rather large contraction from the stable 4L form. This distance is comparable with 2.24 Å, the distance of closest approach in α-Mn metal. It appears likely that 2.27 Å would be too short to prevent the domination of repulsive terms. Unless otherwise disturbed, $SrMnO_3$ assumes the hex 4L structure, apparently as a compromise between the hex 2L and perovskite configurations. The former is more favorable for cation–cation interaction and/or oxygen polarization through total hexagonal stacking while the latter minimizes metal–metal repulsion through total cubic stacking of AO_3 layers. Hex 4L $SrMnO_3$ retains features of both in having alternating cubic and hexagonal stacking.

$SrMnO_{3-x}$ Phases Related to the Hex 4L Structure

Within the 1035–1400°C range, $SrMnO_3$ evolves oxygen, apparently as a result of temperature-dependent reduction of Mn^{4+} to Mn^{3+}. Powder patterns of specimens which were heated >200 h in the above temperature range and rapidly quenched indicate a progressive expansion of cell dimensions with increasing temperature (Fig. 2). The c/a ratio remains essentially constant near 1.666 throughout this temperature range. It is emphasized that specimens must be rapidly quenched to observe the parameter variations. Slow-cooling or "air-quenching" results in rapid reoxidation which, of course, yields the fully oxidized starting material.

The air isobar from 1035–1400°C was located by reoxidizing specimens, at 800°C, which had been previously equilibrated and quenched. Values of x

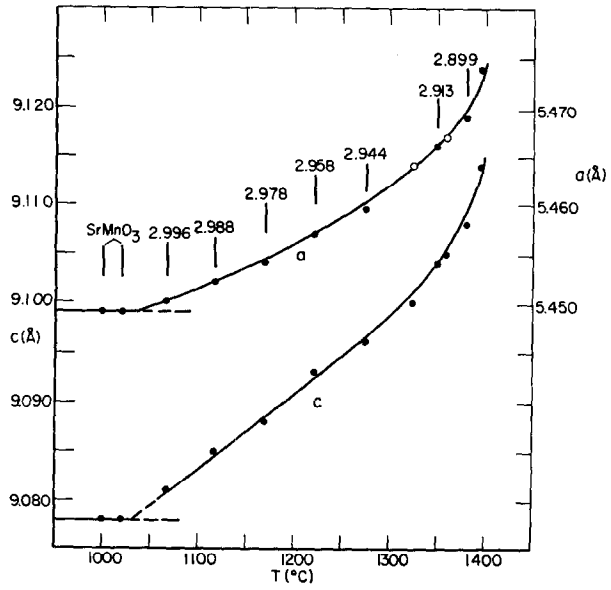

FIG. 2. Variation of room temperature determined cell parameters of 4L $SrMnO_{3-x}$ phases with the temperature from which the phase was quenched. Open circles are the *b* axis of an orthorhombic, distorted hexagonal cell.

were obtained from the weight gains associated with the reaction:

$$SrMnO_{3-x} + \tfrac{1}{2}xO_2 \xrightarrow[\text{air}]{800°C} SrMnO_3.$$

Jonker and Van Santen (*3*) prepared an unknown compound at 1350°C in air corresponding to the composition $SrMnO_{2.925}$. The phase observed at 1350°C and measured in this study is $SrMnO_{2.913}$ which agrees well with the above.

Phases between 1035–1169°C are readily indexed on the basis of hex 4L $SrMnO_3$. Powder patterns of phases between 1222–1400°C, however, show slight line-broadening and over-all loss of intensity indicating poor crystallinity. To improve the crystalline character, a few milligrams of $SrMnO_3$ were (a) heated at 1325°C for 428 h, and (b) heated in a sealed-Pt tube at 1420°C for 1 week, followed by heating in air at 1360°C for 1 week. Both specimens yielded powder patterns which unequivocally show splitting of diffraction lines. The patterns may be indexed on the basis of an orthorhombic distortion of hex 4L $SrMnO_3$, with $a_{orth} \approx a_{hex}\sqrt{3}$, $b_{orth} \approx a_{hex}$; and $c_{orth} = c_{hex}$. The powder pattern for the 1360°C phase, given in Table III, was indexed on the basis of $a = 9.452$ Å, $b = 5.467$ Å, and $c = 9.105$ Å, while the 1325°C phase has $a = 9.456$ Å, $b = 5.464$ Å, and $c = 9.100$ Å. In Fig. 2, the *a* parameter corresponding to 1325 and 1360°C (open circles), therefore, represents the actual *b* parameter of the orthorhombic cell. The slight line-broadening and apparent loss of intensity in the powder patterns of phases between 1222 and 1400°C may be the manifestation of the distortion of the hexagonal cell. Below 1169°C these effects were not observed. This may be reconciled if (a) the distortion below 1169°C is much too small to be detected by X-rays and/or (b) between 1169–1222°C a very narrow two-phase region exists,

TABLE III
X-RAY DIFFRACTION DATA FOR DISTORTED FOUR-LAYER $SrMnO_{3-x}$[a]

d_{obs}	I/I_1[c]	$1/d^2_{calc}$	$1/d^2_{obs}$	hkl[d]
4.728	6	0.0446	0.0447	110
		0.0448		200
3.279	60	0.0929	0.0930	112
		0.0931		202
2.733	100	0.1338	0.1339	020
2.730	80	0.1342	0.1342	310
2.554	50	0.1533	0.1533	113
		0.1533		203
2.289	9	0.1907	0.1909	221
		0.1912		401
2.276	9	0.1930	0.1930	004
2.099	40	0.2269	0.2269	222
2.097	35	0.2273	0.2274	402
2.050	8	0.2377	0.2379	114
		0.2378		204
1.8660	25	0.2872	0.2872	223
1.8646	20	0.2876	0.2876	403
1.6995	4	0.3462	0.3462	115
		0.3463		205
1.6653	8	0.3606	0.3606	132
1.6628	6	0.3615	0.3617	512
1.6404	6	0.3716	0.3716	224
1.5774	12	0.4019	0.4019	330
1.5754	10	0.4029	0.4029	600
1.5414	15	0.4209	0.4209	133
1.5398	9	0.4219	0.4218	513
1.4427	8[e]	0.4702	0.4705	225
		0.4707		405
1.4061	3	0.5054	0.5058	134
		0.5063		514
1.3667	8	0.5354	0.5354	040
1.3648	5	0.5369	0.5369	620

[a] 1360°C, air.
[b] Interplanar spacing (Å).
[c] Relative intensity.
[d] Indexed on the basis of an orthorhombic cell with $a = 9.452$ Å, $b = 5.467$ Å, $c = 9.105$ Å.
[e] Broad.

separating the fields of hex $SrMnO_{3-x}$ and distorted $SrMnO_{3-x}$. The latter (b) would imply that the air isobar between 1035–1400°C consists of two portions separated by a two-phase region. As definitive evidence for (b) was not obtained, the isobar is depicted as a continuous curve. Upon reversal below 1035°C, reduced phases not only reoxidize rapidly but structural distortion is eliminated.

Perovskite Related $SrMnO_{3-x}$ Phases and the Cubic Perovskite $SrMnO_3$

Near 1400°C, the air isobar is discontinuous as the approximate equilibrium

$$SrMnO_{2.89} \underset{\text{air}}{\overset{1400°C}{\longleftrightarrow}} SrMnO_{2.74} + 0.075O_2$$

is established. This very sluggish but reversible reaction represents a structural transition, as well as a change in stoichiometry. The phase $SrMnO_{2.89}$, the limiting member of the "4L structure" homogeneity region, transforms with further reduction, to $SrMnO_{2.74}$, the low-temperature limit of a second homogeneity range characterized by a perovskite-like structure. Phases in this region have the stoichiometry from near $x = 0.26$ to near $x = 0.38$ at the 1740°C melting point. Diffraction patterns of quenched specimens are of poor quality, as individual lines tend to be somewhat broad and diffuse, with $K\alpha_1$–$K\alpha_2$ resolution obscure. Prolonged heating times (>100 h) even at elevated temperatures do not improve the "crystallinity" of specimens. The powder pattern of a typical member of this series, given in Table IV, was indexed on the basis of an orthorhombic distorted perovskite with $a = 5.43$ Å, $b = 3.81$ Å and $c = 5.44$ Å. Cell dimensions were not quantitatively determined because of the poor quality of the diffraction patterns. Increased reduction with increasing temperature, however, may account for the observed expansion of c, contraction of a, and b remaining relatively unaltered. This trend was particularly useful in deducing the direction of the air isobar at the 1740°C melting point. Liquids quenched from above 1740°C yield perovskite-like phases with much larger c values than those just below the melting point [c (1736°C) = 5.45 Å vs c (1744°C) = 5.51 Å]. This suggests that melting proceeds with further reduction rather than oxidation. Bulk compositions of liquids are shown only schematically in Fig. 1, as they were not gravimetrically determined.

TABLE IV
X-RAY DIFFRACTION DATA FOR PEROVSKITE-LIKE $SrMnO_{2.694}$[a]

d_{obs}[b]	I/I_1[c]	$1/d^2_{calc}$	$1/d^2_{obs}$	hkl[d]
3.82	2	0.0677 0.0688	0.0684	101 010
2.721	50	0.1351	0.1350	002
2.716	60	0.1356	0.1356	200
2.707	100	0.1365	0.1364	111
2.214	15	0.2039	0.2039	012
2.211	15	0.2044	0.2045	210
1.922	25	0.2706	0.2705	202
1.905	20	0.2754	0.2755	020
1.568	15	0.4066	0.4066	113
1.566	15	0.4076	0.4078	311
1.560	15	0.4105 0.4110	0.4107	022 220
1.353	10	0.5461	0.5460	222

[a] Prepared at 1525°C, air.
[b] Interplanar spacing, Å.
[c] Relative intensity
[d] Indexed on the basis of an orthorhombic cell with $a = 5.43$ Å, $b = 3.81$ Å, $c = 5.44$ Å.

By decreasing the oxygen pressure and temperature, melting can be avoided and perovskite-like phases with $x > 0.38$ can be prepared. Diffraction patterns of these phases are considerably sharper than those obtained in air but contain additional lines which may reflect an ordering tendency at the lower temperatures and oxygen contents. The subcell parameters a, b, and c reflect a continuation of the variation trend described above. For example, the phase $SrMnO_{2.558}$, prepared by heating for 1 week at 1150°C and 6×10^{-6} atm, has $a = n5.39$ Å, $b = m3.81$ Å, and $c = p5.52$ Å, where n, m, and p are integers describing the supercell. It is not certain whether perovskite-like phases exist to $SrMnO_{2.50}$ or if a limiting, ordered compound $Sr_2Mn_2^{3+}O_5$, similar to $K_2Ti_2O_5$ (*10*), exists at lower oxygen pressures. Attempts to synthesize a $SrMnO_{2.50}$ phase yielded an unknown compound whose powder pattern, given in Table V, could not be indexed either on an orthoperovskite or monoclinic $K_2Ti_2O_5$ basis. Like that of $K_2Ti_2O_5$, the crystallinity of the material deteriorates rapidly while exposed to air at room temperature, perhaps because of reaction with atmospheric moisture. Further low-oxygen pressure-temperature studies should yield information concerning ordered perovskite-like compounds versus disordered nonstoichiometric perovskite phases.

Although the perovskite-like phases quenched from elevated temperatures in air appear poorly crystalline and distorted at room temperature, the true symmetry at elevated temperatures is not known. Furthermore, if "air-cooled" rather than

TABLE V

X-RAY DIFFRACTION DATA FOR UNKNOWN PHASE NEAR $SrMnO_{2.50}$[a]

d_{obs}[b]	I/I_1[c]
3.38	5
2.82	30
2.79	100
2.72	60
2.31	5
2.23	10
2.12	15
2.02	18
1.922	25
1.632	10
1.582	20

[a] Prepared at 1340°C, 1 week, 5×10^{-6} atm.
[b] Interplanar spacing, Å.
[c] Relative intensity.

TABLE VI

X-RAY DIFFRACTION DATA FOR METASTABLE CUBIC $SrMnO_3$ PEROVSKITE

d_{obs}[a]	I/I_1[b]	$1/d^2_{calc}$	$1/d^2_{obs}$	hkl[c]
3.805	4	0.0690	0.0691	100
2.691	100	0.1381	0.1381	110
2.198	26	0.2071	0.2070	111
1.9027	53	0.2762	0.2762	200
1.7022	3	0.3452	0.3451	210
1.5539	46	0.4142	0.4141	211
1.3458	25	0.5523	0.5522	220
1.2036	23	0.6904	0.6903	310
1.1476	8	0.7594	0.7594	311
1.0987	7	0.8285	0.8284	222
1.0172	19	0.9665	0.9665	321
0.9515	13	1.1046	1.1046	400
0.9231	1	1.1737	1.1737	410/322
0.8971	14	1.2427	1.2427	411/330

[a] Interplanar spacing, Å.
[b] Relative intensity.
[c] Indexed on the basis of a cubic cell with $a = 3.806$ Å.

quenched, these phases partially reoxidize and yield diffraction patterns which are extremely difficult to interpret. If allowed to completely reoxidize metastably at low temperature, every distorted perovskite, including those formed in vacuum, converts rapidly to a cubic perovskite which exhibits an exceedingly sharp X-ray pattern. Temperatures as low as 150°C and times as short as 10 min are sufficient. The diffraction pattern of the metastable, cubic perovskite may be indexed on the basis of $a = 3.806$ Å and is given in Table VI.

The possible reaction

$$\underset{\text{cubic perovskite}}{SrMnO_{3-y}} + \tfrac{1}{2}yO_2 \xrightarrow[air]{800°C} \underset{\text{hex 4L}}{SrMnO_3}$$

was measured and found not to involve a weight change ($y = 0$). Gravimetric determinations were thus simplified for the distorted phases by measuring the more rapid reaction

$$\underset{\text{distorted perovskite}}{SrMnO_{3-x}} + \tfrac{1}{2}xO_2 \xrightarrow[0.5\ h]{300°C} \underset{\text{cubic perovskite}}{SrMnO_3}$$

Complete oxidation and transformation of reduced perovskites to hex 4L $SrMnO_3$ requires a 5–20 h treatment in the 800–1000°C range.

Discussion

A qualitative understanding of the equilibrium relations, stability, and structural nature of phases in the system $SrMnO_{3-x}$ is possible by considering the oxidation-reduction equilibrium:

$$2Mn^{4+} + O^{2-} \leftrightarrow 2Mn^{3+} + \tfrac{1}{2}O_2. \qquad (1)$$

This reaction is general and does not necessarily suggest any of the possible, true thermodynamic equilibria which may be operative in the system. Since reduction of Mn^{4+} to Mn^{3+} occurs in the hex 4L structure, Eq. (1) must be considered. Physically, Eq. (1) yields one anion "vacancy" per two Mn^{4+} reduced to the trivalent state. Structurally, the location of the "vacancy" may be within the cubic (A) layers or hexagonal (B, C) layers. Furthermore, the pair of Mn^{4+} formerly bonded to the "missing" oxygen must assume the trivalent state and should have a locally rearranged, unsymmetrical, coordination of remaining anions. If an A-layer oxygen is removed, the corner-sharing of octahedra will be locally disrupted. Similarly, if a B- or C-layer oxygen position is vacant, the face-sharing will be disrupted. The possible local environments which may result are shown in Fig. 3. A missing A-layer anion results in two nonbridging, Mn^{3+} trigonal bipyramids, each sharing a face with a Mn^{4+} octahedron. A missing hexagonal-layer anion creates two distorted Mn^{3+} trigonal bipyramids sharing an edge. These pairs may share corners with similar, adjacent pairs and/or with face-sharing Mn^{4+} pairs. The fivefold coordination suggested is consistent with the stabilization of Mn^{3+} in a trigonal-bipyramidal site through an $e_o^2 e_\pi^2 a_1^0$, configuration of its outer d electrons (*11*).

Blasse(*12*) has suggested that hexagonal structures

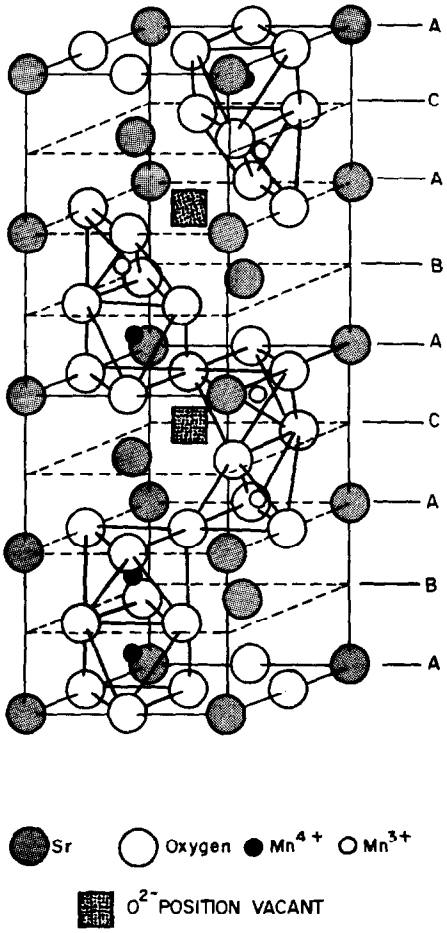

FIG. 3. Two hexagonal four-layer cells indicating the nature of possible environments about Mn^{3+} as a result of (a) a vacant A-layer anion position and (b) a vacant C-(or B)-layer anion position. Trivalent manganese polyhedra are shown without distortion.

of the ABO_3 type are favored by increased oxygen ion polarization, while Katz and Ward (*7*) suggested the possible importance of stabilization through metal–metal *d*-orbital interaction. Regardless of which coordination scheme is considered, as Mn^{3+} pairs are formed through reduction, anion polarization and/or metal–metal interaction are progressively minimized. These can be accompanied by small displacements of the Mn^{3+} (and Mn^{4+}) ions from the $(\frac{1}{3}, \frac{2}{3}, z)$ position of the structure and by slight rearrangement of the remaining oxygens about each Mn^{3+} to achieve a more regular trigonal bipyramidal (rather than square pyramidal) configuration. At low Mn^{3+} concentrations ($x < 0.04$), these phenomena are manifested only by structural expansion. At larger concentrations, the effects are of such great extent as to produce expansion and observable distortion from hexagonal symmetry. The similarity of powder patterns (no apparent superstructure), structural distortion and expansion, with c/a remaining essentially constant, and the ease of reversal to $SrMnO_3$ (<1035°C) of reduced 4L phases, support the proposed model. Within the $0 < x < 0.11$ range the basic or "skeletal" 4L structure remains essentially intact. Reversal to $SrMnO_3$ is easily accomplished by restoring the face-sharing of Mn^{4+} pairs through reoxidation, without gross structural rearrangement.

Under conditions of variable P_{O_2} and temperature, it is unknown to what extent the 4L structure will tolerate mixed octahedral–trigonal bipyramid coordination. The limiting value, $x = 0.11$, in air suggests between four trigonal bipyramids per five ideal 4L cells ($x = 0.10$) and two per two 4L cells ($x = 0.125$) before transformation to a perovskite-like structure occurs. Why this transformation proceeds is also uncertain. Possible solutions may be provided by the concepts of anion polarization and/or metal–metal interaction and of coordination of Mn^{+3} compared with the experimental evidence.

It is well known that hydrostatic pressure tends to increase stability of cubic stacking at elevated temperatures. This is accomplished, presumably, by disruption of face-sharing sequences through increased electrostatic repulsion caused by compression. Eventually, total cubic stacking (a perovskite) may form. Alternatively, reduction of anion polarization and/or metal–metal interaction should produce the same result, given already decreased Mn–Mn distances as in $SrMnO_3$. The Mn^{3+} coordination schemes, previously suggested, may provide the controlling mechanism. If the basic 4L structure were to remain intact to a limiting composition of $Sr_4Mn_4^{3+}O_{10}$ ($x = 0.50$), two different coordination schemes can be generated for Mn^{3+}. Removal of two hexagonal-layer (B, C) oxygens per initial $Sr_4Mn_4O_{12}$ cell produces two edge-sharing pairs of Mn^{3+} trigonal bipyramids linked by corner-sharing. This configuration is highly improbable because (a) structural stabilization through anion polarization is necessarily minimized as the oxygen content is decreased and all manganese is in the trivalent state and/or (b) metal–metal interaction through a shared triangular face of oxygens is totally disrupted. To maintain the 4L structure with a minimum of Mn^{4+} face-sharing pairs and a maximum of Mn^{3+} trigonal bipyramids per cell, removal of only one hexagonal-layer oxygen appears sufficient. The composition $Sr_4Mn_4O_{11}$ ($x = 0.25$) reflects this limiting condition in consisting of a pair of edge-shared Mn^{3+} trigonal bipyramids

corner-sharing with a pair of face-sharing Mn^{4+} octahedra. Similarly, if one cubic-layer oxygen were removed the composition $Sr_4Mn_4O_{11}$ would again be obtained. The resulting coordination scheme would consist of a Mn^{3+} trigonal bipyramid sharing a face with a Mn^{4+} octahedron. This unit shares one corner oxygen per 4L cell with a similar pair. Removal of oxygen beyond this limit while maintaining a basic 4L structure is clearly a difficult process. Trivalent manganese must assume the extraordinary coordination schemes (a) tetrahedral coordination and/or (b) pairs of face-sharing Mn^{3+} trigonal bipyramids.

Regardless of which coordination scheme is assumed, a limiting composition for the 4L structure appears to be near $x = 0.25$. Removal of hexagonal-layer oxygens beyond one per 4L cell minimizes the stabilization effects of anion polarization and/or metal–metal interaction, while improbable coordination schemes for Mn^{3+} result if cubic-layer oxygens are missing beyond this limit. For either case, a change in the sharing of polyhedral elements through an appropriate structural transformation is preferable before further removal of anions. It is, consequently, suggested that the basic 4L structure remains stable as the number of missing oxygens approaches one per ideal 4L cell, at which point a sluggish transformation to a perovskite must occur. This limiting condition is shown in Fig. 4. In Fig. 4a, three ideal 4L cells are shown

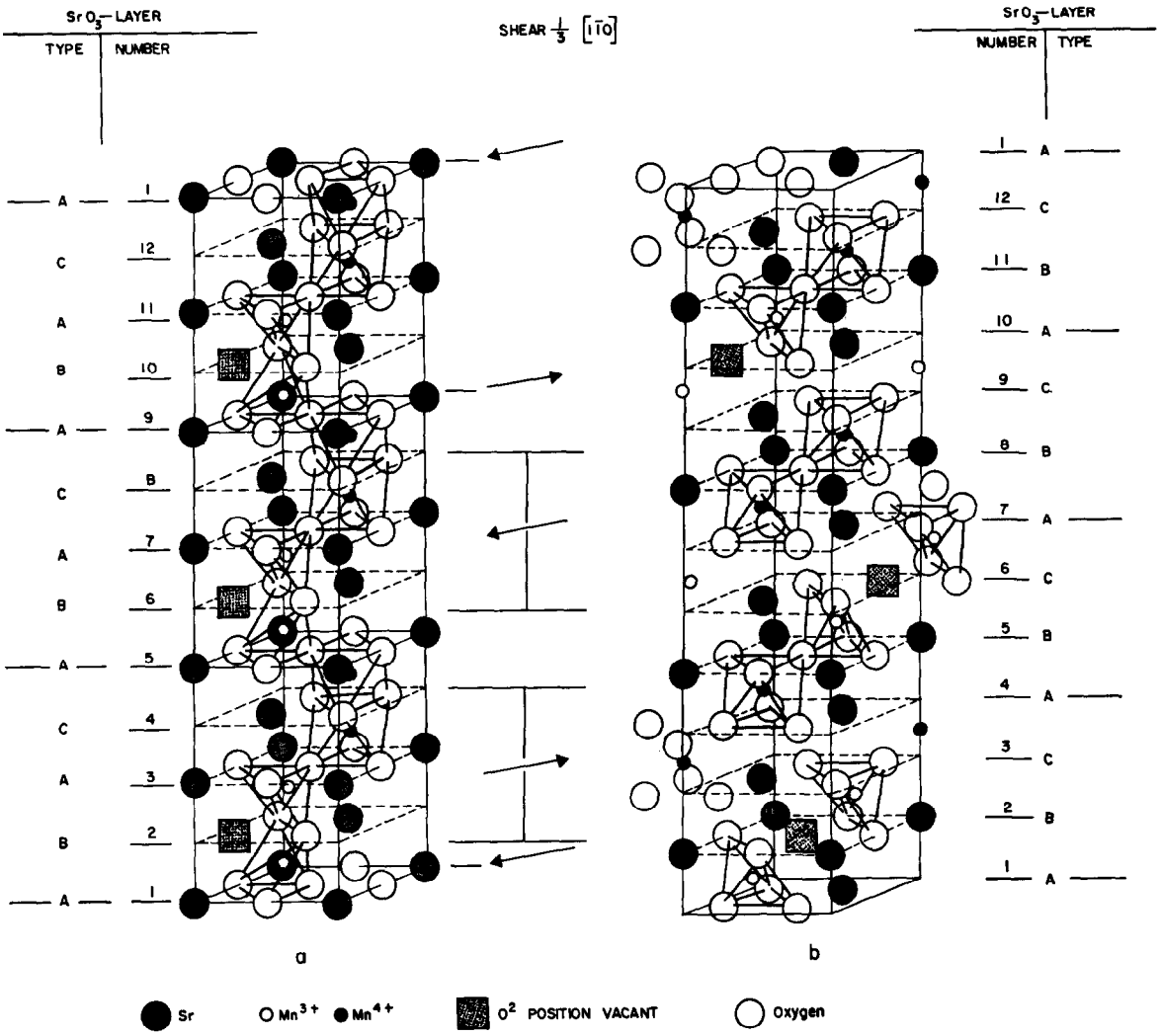

FIG. 4. Transformation of a four-layer (ABAC sequence) structure to a perovskite (ABC sequence) by shearing parallel to (110). (a) Three idealized four-layer cells of bulk composition $Sr_{12}Mn_{12}O_{33}$ with hexagonal layer oxygens missing. (b) Four idealized, three-layer perovskite units with bulk composition $Sr_{12}Mn_{12}O_{33}$. All manganese cations are not shown.

having the limiting bulk composition $Sr_{12}Mn_{12}O_{33}$ ($x = 0.25$) with hexagonal-layer O^{2-} missing. Transformation to a perovskite of the same composition can occur by "shearing" parallel to (110). The minimum number of shears, $\frac{1}{3}$ [1$\bar{1}$0], required to produce total cubic stacking (i.e., four, three-layer perovskite cells on a hexagonal basis) is also depicted. Two initially cubic A-layers and two initial BAC-sequence blocks per 12 layers must shear in opposing directions. The BAC-blocks need not be disrupted internally as they are perovskite-like entities initially. The resulting perovskite-like phase (Fig. 4b) will consist, within the vicinity of each missing oxygen, of nonbridging Mn^{3+} trigonal bipyramids sharing corners with Mn^{4+} octahedra. The maximum oxygen content should be near $Sr_{12}Mn_{12}O_{33}$ or $SrMnO_{2.75}$. (The same mechanism proposed would also be applicable for a 4L $SrMnO_3$ to perovskite transformation under pressure.) It is noted that the perovskite at the 1400°C, air, transition is near $SrMnO_{2.74}$ almost corresponding with that given by the above hypothesis.

If stoichiometry, with its direct effects on the coordination of manganese, anion polarization, and metal–metal interaction, is responsible for the structural transformation, the solvus curve between the 4L structure and the two-phase equilibrium can have some slope. The solvus curve, however, between the "perovskite" and the two phase equilibrium should be almost vertical over a given oxygen-pressure region. Proof of this must await varied oxygen-pressure experimental data.

Once in a "perovskite-like" configuration, the structure can lose further oxygen with increasing temperature. This can be accomplished by the continuous removal of corner oxygens shared by available Mn^{4+} octahedral pairs and the formation of nonbridging Mn^{3+} trigonal bipyramids. As might be expected, quenched specimens of the perovskite-like phases yield diffraction patterns of poor quality, suggestive of a highly disordered, poorly crystalline material. That these phases are truly perovskite in nature, contain Mn^{3+} trigonal bipyramids and do not consist of face-shared structural elements of the 4L structure, are strongly supported by the ease and extreme rapidity of low-temperature reoxidation to a metastable, stoichiometric, cubic perovskite. The transformation of nonbridging Mn^{3+} trigonal bipyramids to corner-shared Mn^{4+} octahedra, especially at the lower temperatures in what may be considered a "skeletal" perovskite is a simple, rapid process compared to the structural rearrangement required for conversion to the 4L phase. Reversal does occur, however, given sufficient time below 1035°C.

The nature and temperature-dependent stability of the polyhedral ordering which appears to exist in phases of low-oxygen content at lower oxygen pressures should be further investigated.

References

1. A. D. WADSLEY, *in* "Non-Stoichiometric Compounds" (L. Mandelcorn, Ed.), Chap. 3, Academic Press Inc., New York, 1964.
2. E. W. GORTER, *Proc. Intern. Congr. Pure Appl. Chem. 17th* **1**, 303 (1959).
3. G. H. JONKER AND J. H. VAN SANTEN, *Physica* **16**, 337 (1950).
4. J. B. MACCHESNEY, H. J. WILLIAMS, J. F. POTTER, AND R. C. SHERWOOD, *Phys. Rev.* **164**, 779 (1967).
5. S. J. SCHNEIDER AND J. L. WARING, *J. Res. Natl. Bur. Std.* **67A**, 19 (1963).
6. A. HARDY, *Acta Cryst.* **15**, 179 (1962).
7. L. KATZ AND R. WARD, *Inorg. Chem.* **3**, 205 (1964).
8. J. J. LANDER, *Acta Cryst.* **4**, 148 (1951).
9. B. E. GUSHEE, L. KATZ, AND R. WARD, *J. Amer. Chem. Soc.* **79**, 5601 (1957).
10. S. ANDERSSON AND A. D. WADSLEY, *Nature* **187**, 499 (1960).
11. J. B. GOODENOUGH AND J. M. LONGO, "Crystallographic and Magnetic Properties of Perovskite and Perovskite-Related Compounds." To be published.
12. G. BLASSE, *Inorg. Nucl. Chem.* **27**, 993 (1965).